http://dx.doi.org/10.21611/qirt.2014.011

Time-resolved Thermal Infrared Multispectral Imaging of Gases and Minerals

Marc-André Gagnon, Karl-Alexandre Jahjah, Frédéric Marcotte, Pierre Tremblay, Vincent Farley and Martin Chamberland*
Telops, 100-2600 Saint-Jean Baptiste, Québec, QC, Canada G2E 6J5

ABSTRACT

For years, scientists have used thermal broadband cameras to perform target characterization in the longwave (LWIR) and midwave (MWIR) infrared spectral bands. The analysis of broadband imaging sequences typically provides energy, morphological and/or spatiotemporal information. However, there is very little information about the chemical nature of the investigated targets when using such systems due to the lack of spectral content in the images. In order to improve the outcomes of these studies, Telops has developed dynamic multispectral imaging systems which allow synchronized acquisition on 8 channels, at a high frame rate, using a motorized filter wheel. An overview of the technology is presented in this work as well as results from measurements of solvent vapors and minerals. Time-resolved multispectral imaging carried out with the Telops system illustrates the benefits of spectral information obtained at a high frame rate when facing situations involving dynamic events such as gas cloud dispersion. Comparison of the results obtained using the information from the different acquisition channels with the corresponding broadband infrared images illustrates the selectivity enabled by multispectral imaging for characterization of gas and solid targets.

Keywords: Multispectral, infrared camera, thermal imaging, filter wheel, standoff detection, remote sensing.

1. INTRODUCTION

Thermal infrared (8-12 μm) imaging has been used for many years for the characterization of solid targets and gas clouds. Self-emission, inherent to thermal infrared, makes this spectral range very attractive over others as information can be obtained in various illumination conditions. Spatial contrasts in thermal infrared images result from temperature or emissivity differences between neighboring objects. For gases, contrast is typically defined relative to its background while irradiance from the hemispheric environment is the typical frame of reference for solids. The sensitivity and accuracy of modern thermal infrared systems allows measurement of very small thermal contrast, at high spatial resolution, fast frame rate and on a wide dynamic range. In order to retrieve the most out of imaging sequences, different image processing strategies are used. Morphological analyses deal with pattern recognition within images. Target detection is carried out by matching shapes/energy with thermal signature of known objects such as flares, decoys and ship plumes. Temporal analysis exploits the thermal differences in space as a function of time.[1] Change detection algorithms are routinely used to detect the presence of dispersing infrared-active gas clouds in a scene. Despite all these efforts, broadband thermal infrared systems bring limited information about the chemical nature of the targets. For such systems, the response of each pixel results from the sum, over a fixed spectral range, of all contributions, from all objects in a scene, regardless of their chemical nature. It is well known that most chemicals selectively absorb/emit infrared radiation at discrete energies, i.e. very narrow spectral ranges. Consequently, the minor contributions of gas/solid targets to the overall signal recorded by an infrared detector translate into very small thermal contrasts. The absorption pattern of gases and solids as a function of wavelengths (or wavenumbers) is referred to as its infrared spectral signature. In the case of gases, infrared radiation from their background is selectively absorbed and re-emitted in a very unique fashion. For solid targets like polymers, minerals and organic and inorganic salts, both self-emission and reflection occur at wavelengths which depend on their chemical nature. Selectivity concerns rapidly arise when dealing with simultaneous detection of targets of different chemical nature. Therefore, it is very challenging to infer the nature of a target based on broadband imaging, especially when chemicals have similar spectral features. Information on the spectral dimension is typically required to achieve efficient and selective detection of targets from infrared imaging sequences. For dynamic

* martin.chamberland@telops.com; phone +1-418-864-7808; fax +1-418-864-7843; www.telops.com

http://dx.doi.org/10.21611/qirt.2014.011

events such as gas cloud dispersions and/or combustions of energetic material, it is preferable that such information be obtained without scarifying the imaging frame rate.

In order to acquire spectral information using thermal infrared cameras, tuning of the detectors' spectral response is typically achieved using spectral filters. Band-pass (BP), long-pass (LP) and high-pass (HP) spectral filters are commercially available and can be readily added in the cameras' optical path. For cooled infrared cameras, narrowband imaging can be achieved by installing a BP filter directly in the detector assembly. Cold filters provide high sensitivity, but are typically designed to address very specific applications since they cannot be easily changed (permanent) in most cases. In order to get more flexibility, interchangeable filters, at ambient temperature, can be added in the cameras' optical path. Whether the filter is cold or at ambient temperature, its spectral range must be selected with great care since no filter change can be made without stopping the acquisition and/or redoing a radiometric calibration. For this reason, filter wheel systems have gained popularity since they allow to store a selection of spectral filters readily available for acquisition. Multispectral imaging consists in acquiring multiple images of the same scene using the different spectral filters and this represents a great compromise between broadband imaging and hyperspectral imaging.[2] Spectral information can be obtained from the response of individual spectral filters, ratios, subtractions and/or combinations of multiple filters. In general, a greater number of spectral bands provide more flexibility to face challenging situations. Despite the obvious advantages of thermal infrared multispectral imaging, the low acquisition rate, i.e. spectral band rate, of most commercially available systems make their use less appealing than conventional imaging systems. In most of these systems, the filter wheel is not rotating during image acquisition. The selection and/or spectral filter change must be made between each acquisition sequence. Such operation mode is somewhat incompatible with non-stationary scenes (e.g. gas cloud dispersion, combustions, flares…). In addition, the limited number of available spectral filters (typically 4) provides low spectral resolution, thus low selectivity.

The Telops MS-IR infrared camera series performs dynamic multispectral imaging, at a high frame rate, on 8 channels using a fast-rotating filter wheel. In order to perform time-resolved multispectral imaging, the filter wheel is driven synchronously with the FPA clocking such that a single frame is recorded at each filter position. Sequences are then calibrated using in-band photon radiance (IBR) format, frame by frame, according to their respective spectral filter dataset. In order to illustrate the capabilities of this system, time-resolved multispectral imaging of gases and solids was carried out using a combination of 7 spectral filters and 1 neutral density filter with the MS-IR VLW camera (very longwave 7.7 – 11.8 μm). Imaging of methanol vapors was first carried out to illustrate how thermal contrast can be enhanced by selecting spectral filters which match the absorption bands of a target. Multispectral imaging of a freely dispersing gas cloud, carried out at a frame rate of 30 Hz/channel, clearly illustrates the benefits of dynamic multispectral imaging, such as the one developed by Telops, over more conventional stationary filter wheel systems. Multispectral imaging of minerals was then carried out to illustrate the versatility of this camera. For both gases and solids, IBR profile correlation was applied to the multispectral imaging sequences to enhance thermal contrast based on spectral information. In each case, comparison with corresponding broadband image illustrates the selectivity enabled by dynamic multispectral imaging.

2. EXPERIMENTAL SECTION

2.1 MS-IR Infrared Cameras Series

Telops MS-IR imaging systems are high performance cooled multispectral infrared cameras available in different models covering the complete mid-infrared spectral range. The MS-IR MW (midwave, 3.0 – 4.9 μm) and MS-IR VLW (very longwave 7.7 – 11.8 μm) use 640×512 pixels InSb and 320×256 pixels MCT (Mercury-Cadmium-Telluride) focal plane array (FPA) detectors respectively. The MS-IR-HD is the midwave version which uses a high-definition 1280×1024 pixels FPA detector. The MS-IR-FAST is a fast 320×256 pixels FPA detector which allows image acquisition at the highest frame rate available. The MS-IR infrared cameras allow splitting of the scene radiance into eight different spectral bands rather than only one broadband image hereby providing spectral information about the investigated targets. The filter wheel is a fast rotating mechanism designed to maximize the camera's frame rate and can be used either in fixed or rotating mode. The filter wheel is capable of reaching up to 6000 rpm (revolutions per minute), leading to a maximum effective frame rate of 800 Hz, i.e. 100 Hz per channel. All cameras from the MS-IR series benefit from the real-time radiometric and non-uniformity correction features using Telops patented blackbody free correction method.[3]

http://dx.doi.org/10.21611/qirt.2014.011

Figure 1 Telops MS-IR infrared camera (left) and filter wheel system (right).

2.2 Experimental Setup

In order to provide spectral information, 8 different filters were used and their corresponding transmittance curves, convolved with the FPA detectors' spectral response, are reported in Figure 2. Channel #1 was occupied by a neutral density filter and the associated frames are representative of broadband images.

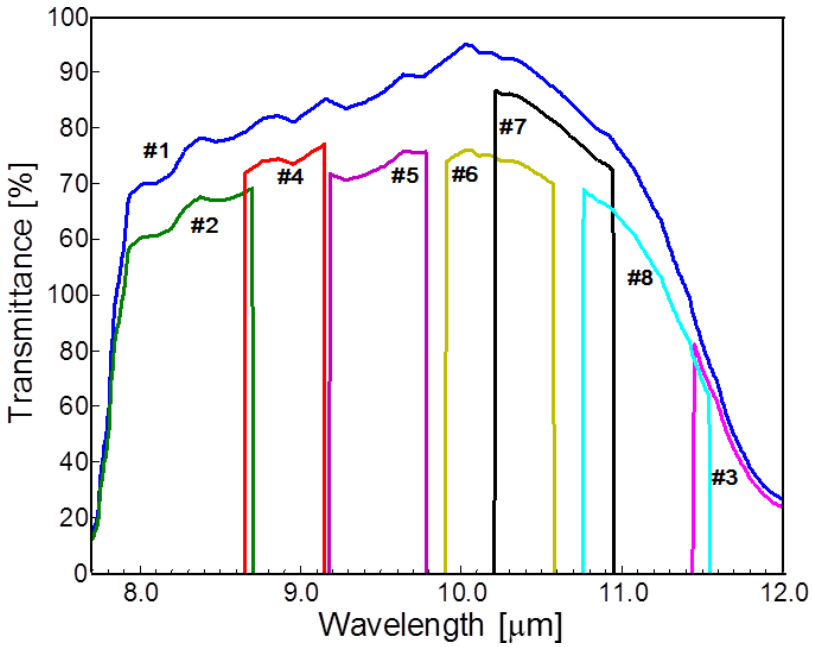

Figure 2 Spectral transmittance of the different filters. Filter #1 (blue curve) neutral density filter/broadband, filter#2 (green curve) SP 8.7 μm, filter #3 (pink curve) LP 11.3 μm, filter#4 (red curve) BP 8.9 μm, filter #5 (purple curve) BP 9.48 μm, filter #6 (dark yellow curve) BP 10.24 μm, filter #7 (black curve) BP 10.58 μm and filter #8 (turquoise curve) BP 11.16 μm.

Acquisitions were carried out using the full FPA frame, i.e. 320×256 pixels, using integration times ranging from 195 to 400 μs depending on the spectral filter. The filter wheel rotation speed was set to 1800 rpm leading to an effective frame rate of 30 Hz/filter. A circular 50 mm Janos Varia lens was used for all experiments. The camera was installed at a distance of 2 m from the targets leading to a spatial resolution of 4 mm^2/pixel. All experiments were carried out indoor at an ambient temperature of about 20°C. Pure methanol was poured in a recipient and the liquid was set on fire. After a few minutes, the flame was extinguished and warm methanol vapors were allowed to freely disperse as a result of vapor pressure. A hematite (Fe_2O_3) drill core contaminated with quartz (SiO_2) veins, iron pyrite (FeS_2) and amethyst minerals were placed in oven set to 150 °C for few minutes. The minerals were then placed on a table and multispectral sequences were readily recorded.

http://dx.doi.org/10.21611/qirt.2014.011

2.3 Image Processing

Spectral filters typically transmit radiance over relatively wide spectral ranges. Radiometric calibration of multispectral cameras consists in characterizing the detector and its optical components responses against known radiance values. Therefore, the IBR procedure mostly consists in integrating the Planck curve equation over a finite spectral range, i.e. the one corresponding to each filter. The IBR of a selected target can be estimated for each filter according to its spectral emissivity for defined concentration and thermal contrast conditions. Thermal contrast can then be enhanced, for a selected target, by correlating its estimated IBR profile with measured IBR profiles of individual pixels in a scene.

3. RESULTS AND DISCUSSION

3.1 Solvent Vapors

In order to illustrate the selectivity provided by dynamic multispectral imaging, experiments were first carried out on warm methanol vapors. Methanol selectively absorbs/emits infrared radiation at discrete energies as represented by its gas-phase absorption spectrum in Figure 3.

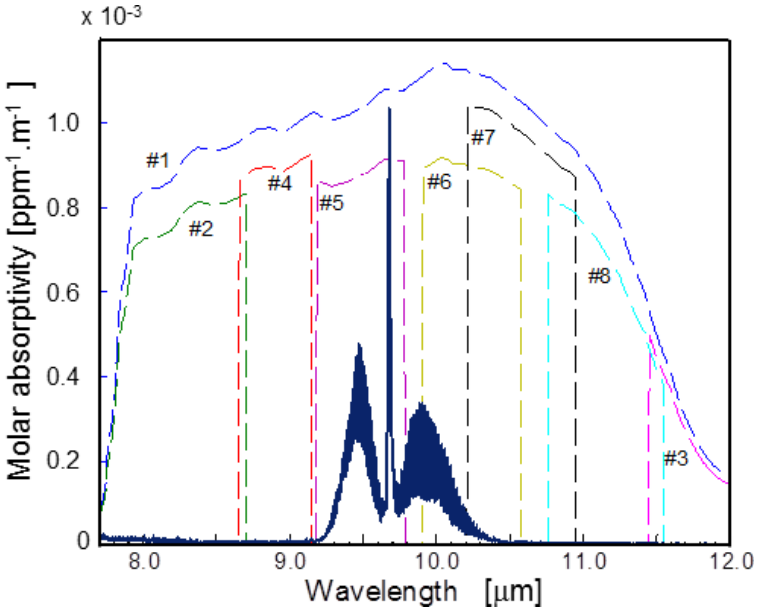

Figure 3 LWIR infrared spectrum of gas-phase methanol (dark blue curve). The transmittance curves of each spectral filter used for the experiment are shown for evaluation purposes.

As seen in Figure 3, absorption/emission of LWIR radiation mostly occurs in the 9.1 – 10.2 µm spectral range due to a spectral feature associated with the C-OH stretch vibration mode of methanol. Consequently, the greatest thermal contrast should be obtained through filters #5 and #6. To illustrate how a selective absorber/emitter of infrared radiation, such as methanol, behaves toward thermal infrared camera systems, a short imaging sequence showing the individual response of each acquisition channel is shown in Figure 4. During this short period of time of about 130 ms, the motorized filter wheel completed 4 full revolutions. In order to compare the response of each individual filter with one another, each IBR was normalized with the corresponding IBR of a blackbody source at 65 °C (which corresponds to methanol boiling point). This normalization procedure allows evaluating, on a mutual basis, the potential of each spectral filter to investigate a specific target. As seen in Figure 4, values of 0.5 and 1.5 were obtained, through each spectral filter, for the background wall and the solvent recipient respectively. This suggests that both objects behave like grey bodies, i.e. have a constant emissivity value in the investigated spectral range, and that the background wall and solvent recipient are much colder and warmer than 65 °C respectively. The typical behavior of a selective absorber/emitter of infrared radiation can be readily seen in Figure 4 as thermal contrast associated with the methanol vapors can be seen on some, but not all, acquisition channels. As expected, the greatest thermal contrast is obtained through filters #5 and #6 which match the spectral features of methanol gas. In this case, the methanol vapors are warmer than their background. Therefore, infrared self-emission from methanol is greater than infrared absorption of the background irradiance and a

http://dx.doi.org/10.21611/qirt.2014.011

positive thermal contrast is obtained. The relative responses of the other spectral filters are also in good agreement with the infrared methanol spectral signature. Almost no thermal contrast associated with methanol vapors can be seen in images recorded through filters #3, #4, #7 and #8 since methanol transmittance is close to 100 % (absorption close to 0) in these spectral channels. The neutral density filter (channel #1) is representative of a broadband image obtained with conventional LWIR cameras. A thermal contrast can be seen in the broadband images which is however not as great as the one obtained through filters #5 and #6. This can be rationalized by the minor contribution of methanol, for which the spectral features cover about one third of the detector spectral range, to the overall radiance measured by a LWIR broadband camera.

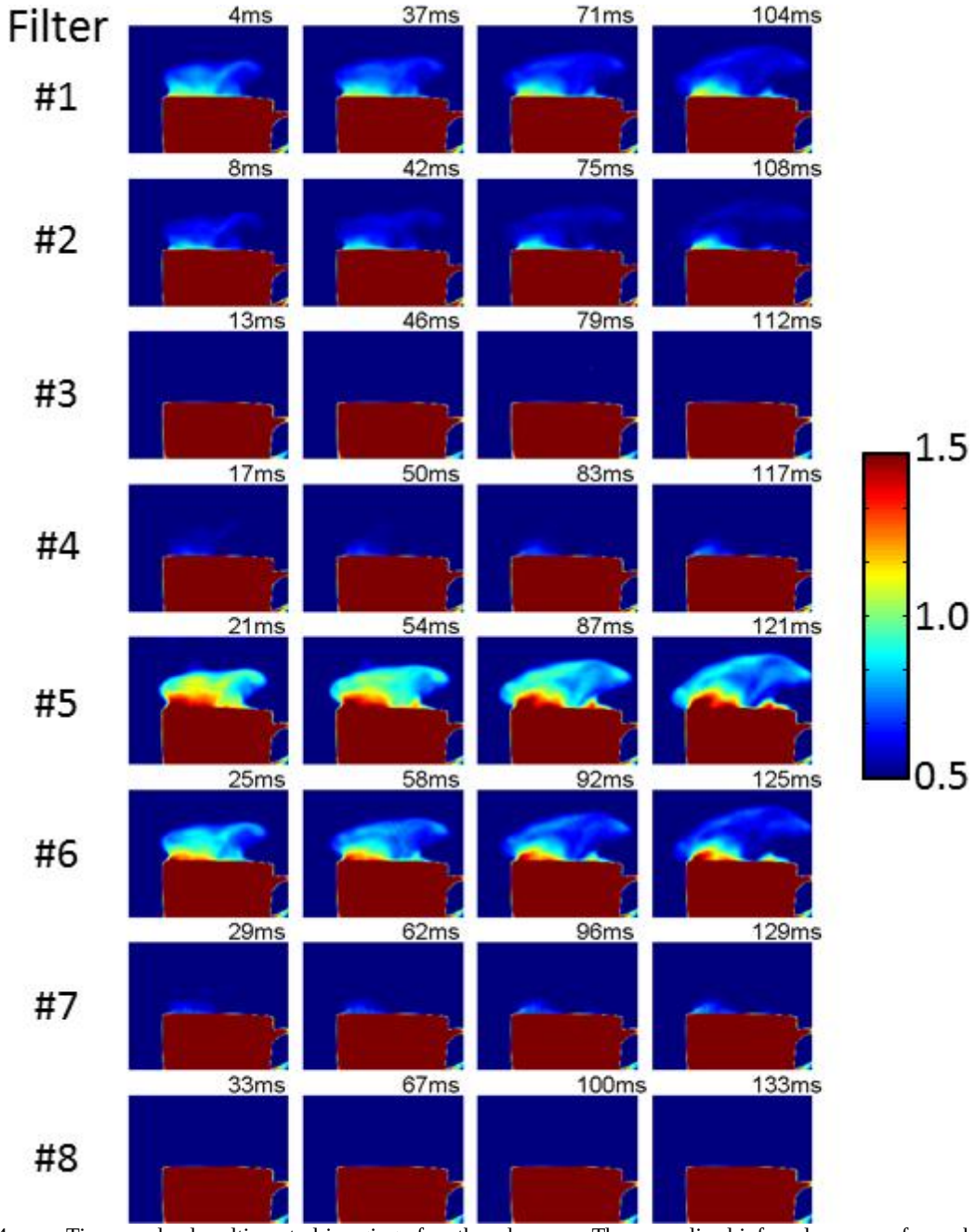

Figure 4 Time-resolved multispectral imaging of methanol vapors. The normalized infrared response for each filter is presented for 4 successive measurements. The associated time stamp of each frame is displayed to highlight the high frame rate acquisition.

http://dx.doi.org/10.21611/qirt.2014.011

From broadband infrared imaging, it is difficult to obtain information about the chemical nature of targets in a scene due to the lack of spectral information. As seen in Figure 3 and Figure 4, the raw spectral information provided by the thermal contrast measured in the different channels brings some additional information about chemical nature of a target. However, one must not solely rely on the presence/absence of thermal contrast in a specific spectral channel to identify a target in a scene. The detector response in a single channel is function of many parameters and is also subject to interfering agents. In order to enhance contrast in a scene relative to a target of interest, image correlation of its IBR profile is carried out. To illustrate this procedure, the IBR profile of a blackbody source and methanol vapor at 65 °C were estimated, according to their absorption features, and the results are shown in Figure 5. The measured IBR profile of pixels located above the methanol recipient is also shown in Figure 5. The similarity between the estimated IBR profile of methanol and the measurement can be readily seen and discriminated from a blackbody source.

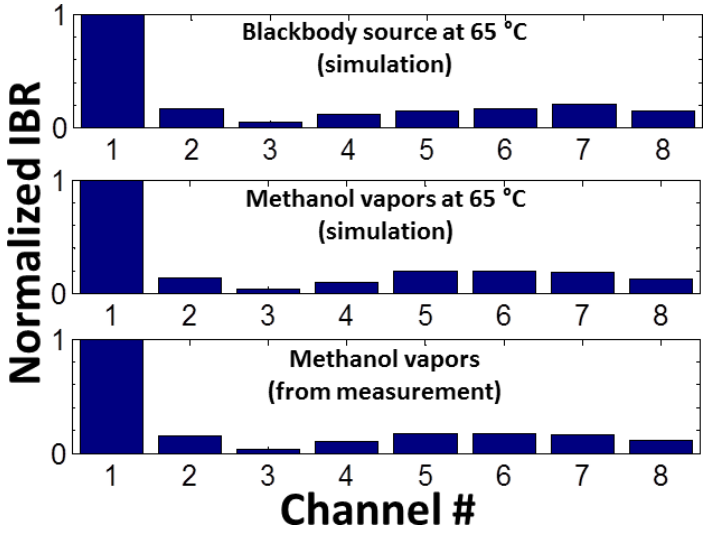

Figure 5 In-band radiance (IBR) profiles estimated for a blackbody source (top) and warm methanol vapors (middle) as well as the measured IBR profile of selected pixels associated with methanol vapors (bottom).

Image correlation based on the IBR profile of warm methanol vapor was then carried out and the results are shown in Figure 6. It can be seen that the image contrast is highly representative of the spatial distribution of methanol vapors in the scene. Surprisingly, a lower correlation value is obtained for a region located right above the recipient as shown by the black arrow in Figure 6. According to the images from filters #5 and #6 in Figure 4, methanol vapors are expected to be present at a high concentration. What first appears as an inconsistency can be explained on the basis of IBR profile differences between the two concentrations and/or temperature regimes of methanol vapors. The estimation of IBR profile is carried out with temperature and concentration assumptions. For very high concentrations, the absorption spectrum distorts, in a non-linear fashion, as a function of concentration. This impacts the IBR profile and indisputably the correlation results. Nevertheless, the spectral information brought by multispectral imaging allows distinguishing efficiently a target of interest from its background and other objects in a scene. In addition, it can be seen in Figure 6 that this information is obtained at a relatively high frame rate. Even slight movements of the methanol gas cloud can be tracked using time-resolved multispectral imaging. Larger changes can be seen on the complete correlation image video sequence. Comparison with the corresponding broadband image video sequence, i.e. from acquisition channel #1, clearly illustrate the benefits of time-resolve multispectral imaging for characterization of dynamic events involving selective absorber/emitter of thermal infrared radiation (see Video 1 and Video 2).

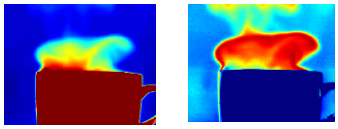

Video 1 "Methanol_Broadband_sequence.wmv" Broadband infrared video sequence of methanol vapors displayed at 30 Hz. "http://dx.doi.org/doi.number.goes.here"

Video 2 "Methanol_Correlation_Image_sequence.wmv" Correlation image video sequence of methanol vapors displayed at 30 Hz. "http://dx.doi.org/doi.number.goes.here"

http://dx.doi.org/10.21611/qirt.2014.011

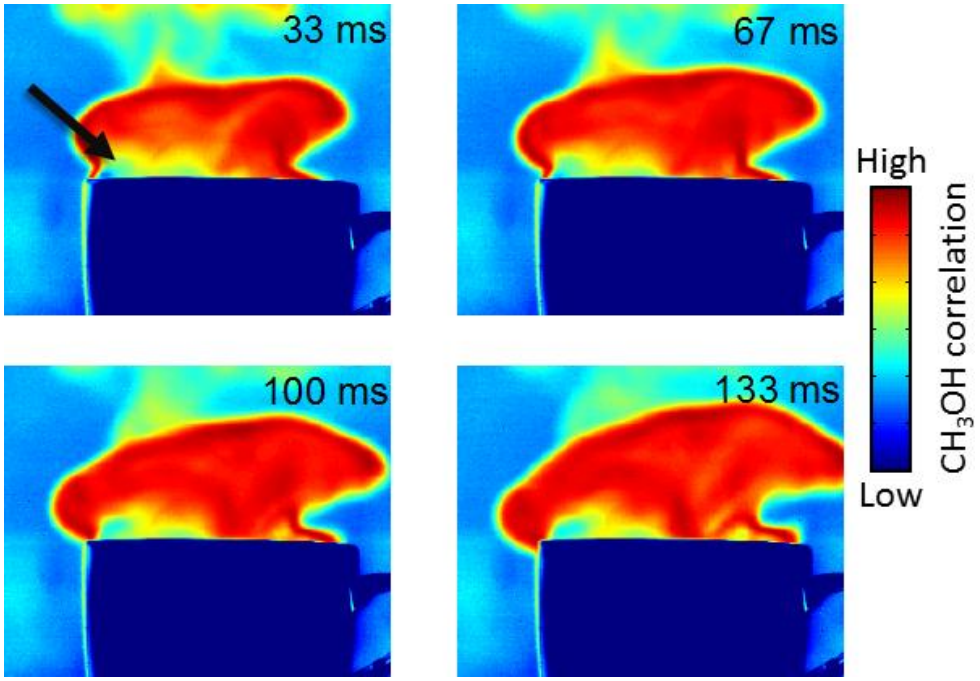

Figure 6 Correlation images of methanol vapors obtained from its IBR profile.

3.2 Minerals

Multispectral imaging of minerals was carried out to illustrate how spectral information can benefit the characterization of solid targets for which the emissivity varies as a function of wavelength. A visible image of the experimental setup is shown in Figure 7. The hematite drill core appears fairly homogeneous except for a few obvious quartz veins.

Figure 7 Visible image of a hematite drill core contaminated with quartz veins (left), iron pyrite (center) and amethyst (right).

Hematite has no appreciable spectral features in the LWIR. Therefore, it is expected to behave like a grey body. Amethyst is a quartz variety doped with iron (Fe) molecules and its spectral emissivity pattern is similar to quartz. It should be noted that the exposed surface of the amethyst mineral in the experiment is essentially a group of «pure» quartz crystals. The emissivity spectrum of quartz is represented in Figure 8 as well as the transmittance curves of each spectral filter.

http://dx.doi.org/10.21611/qirt.2014.011

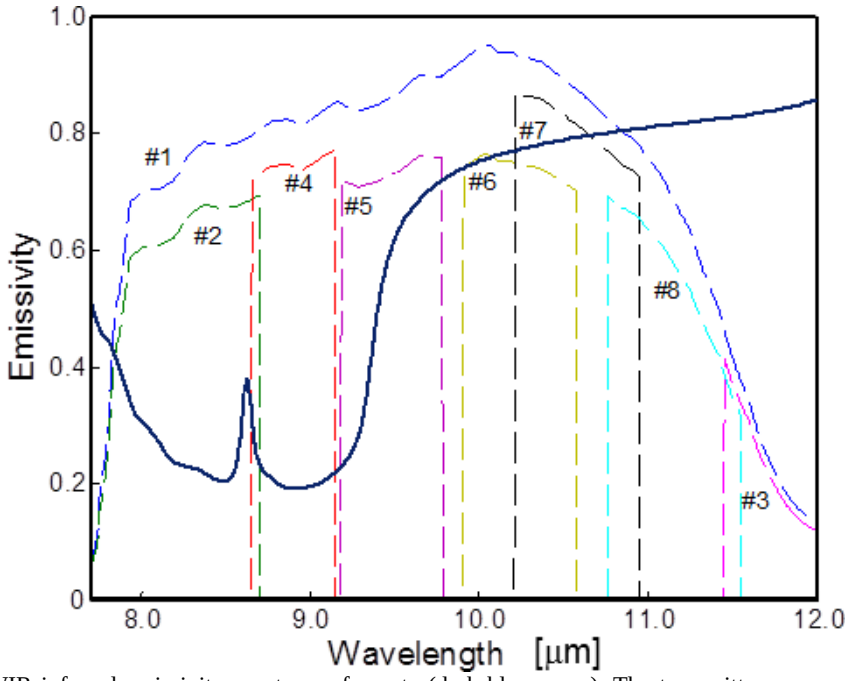

Figure 8 LWIR infrared emissivity spectrum of quartz (dark blue curve). The transmittance curves of each spectral filter used for the experiment are shown for comparison purposes.

As seen in Figure 8, the emissivity of quartz is lower within the 7.7 – 9.6 μm spectral range, a spectral feature associated with the Si-O stretch vibration mode of quartz. For minerals (and solid targets in general), lower emissivity translates into higher reflection. In this case, irradiance, i.e. the total incident power from a hemisphere on the mineral, corresponds to self-emission from the colder walls and ceiling of the room. Therefore, quartz should appear as «colder» in this spectral range. In the 9.6 – 12 μm range, quartz is expected to behave like a blackbody source and its self-emission will be function of its temperature as expressed by the Planck equation. From Figure 8, it can be assumed that the most potent spectral bands for quartz characterization correspond to filters #2, #4 and #5. The individual response of each acquisition channel is shown in Figure 9 on a normalized scale. In order to compare the response of each individual filter with one another, each IBR was normalized with the corresponding IBR of a blackbody source set to an arbitrary temperature of 90 °C. This normalization procedure allows to evaluate, on a mutual basis, the potential of each spectral filter to characterize a specific target.

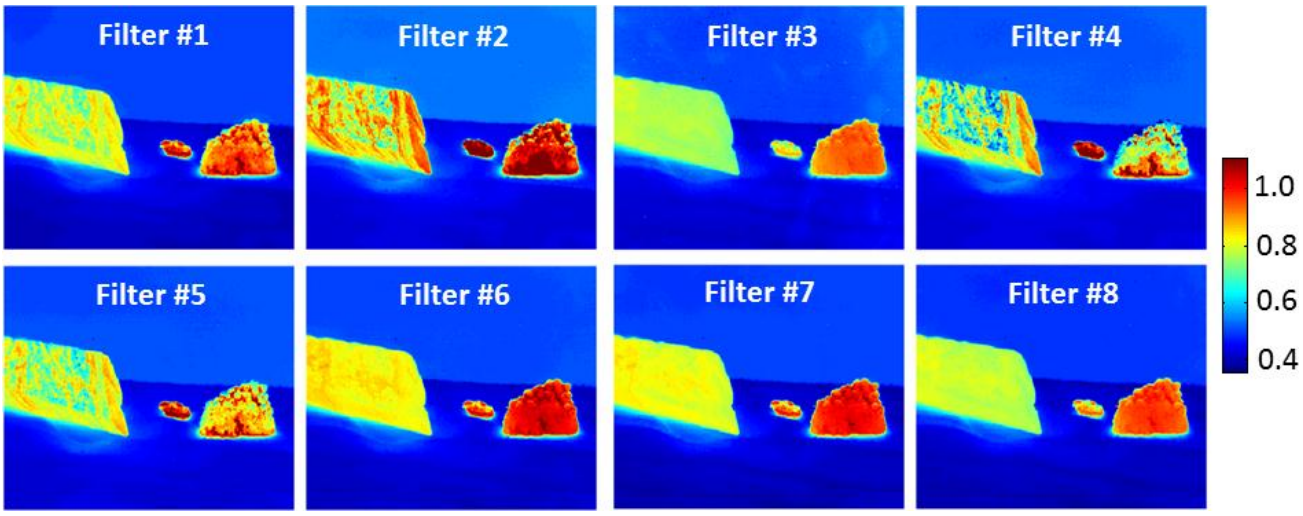

Figure 9 Normalized response (blackbody source of 90 °C) of individual channels for multispectral imaging experiment on minerals.

http://dx.doi.org/10.21611/qirt.2014.011

As seen in Figure 9, similar responses through all spectral filters were obtained for the background wall and the table. This suggests that both objects behave like grey bodies, i.e. have a constant emissivity value in the investigated spectral range. The emissivity dependency of quartz as a function of wavelength can be readily seen in Figure 9 as thermal contrast associated with quartz minerals is different in all acquisition channels. As expected, contrasts on the hematite surface can mostly be seen through filters #2, #4 and #5 as a result of the presence of quartz. From the infrared images, quartz appears to be sparsely dispersed throughout the whole hematite drill core and much more than the visible image suggests. A similar spectral filter response trend is observed for the amethyst mineral with the exception of filter #2 where the signal is higher than expected. Evaluation of the different spectral bands through a normalization procedure is subject to contrast variations which depend on the normalization factor. As seen in Figure 10, there is a significant temperature difference between the hematite drill core and the amethyst mineral.

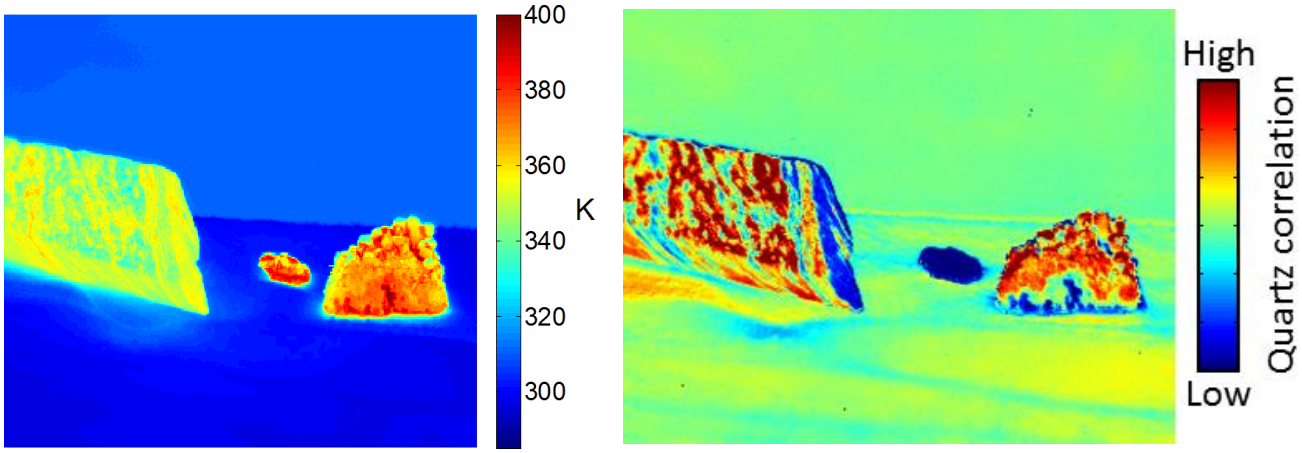

Figure 10 Radiometric temperature image (left) of the experimental setup on minerals and the corresponding correlation images (right) obtained from the IBR profile of quartz.

The correlation image calculated from the IBR profile of quartz is also shown in Figure 10. The contrasts in the image are highly representative of the spatial distribution of quartz through the minerals. Multiple quartz veins can be seen on the surface of the hematite dill core. As expected, the amethyst crystals at the surface of the mineral strongly correlate with quartz IBR profile. The lower correlation obtained for the iron pyrite mineral illustrates the selectivity provided by multispectral imaging over broadband imaging. The correlation procedure also has the advantage of being much less sensitive to temperature differences between similar targets (as seen in Figure 9) for target characterization. Both the hematite drill core and amethyst minerals have the same spectral features associated with quartz, but are at very different temperatures. The spectral information provided by multispectral imaging allows contrast enhancements based on spectral emissivity and not only self-emission. Comparison of the correlation image with the temperature image (Figure 10) clearly highlights this point.

4. CONCLUSION

Time-resolved multispectral imaging allows efficient characterization of dynamic phenomenon such as gas cloud dispersion. The Telops multispectral imaging system provides spectral information without sacrificing the imaging frame rate required in such situations. IBR profiles drawn from 8 acquisition channels provide good information for image contrast enhancement of both gas and solid targets. Comparison between the correlation images, obtained from multispectral imaging, and their associated broadband image illustrates the usefulness of IBR profile analysis to discriminate emissivity differences from temperature differences. The additional information brought by dynamic multispectral imaging over conventional thermal cameras brings new possibilities for infrared signature measurements.

http://dx.doi.org/10.21611/qirt.2014.011

5. REFERENCES

[1] C. Ibarra-Castanedo et al., "Water ingress detection in honeycomb sandwich panels by passive infrared thermography using a high resolution thermal imaging camera, " Proc. of SPIE, 7673, 766212-1 (2012).

[2] Pierre Tremblay et al., "Standoff Gas Identification and Quantification from Turbulent Stack Plumes with an Imaging Fourier-transformed Spectrometer," Proc. of SPIE, 7673, 76730H (2010).

[3] Pierre Tremblay et al., "Pixel-wise real-time advanced calibration method for thermal infrared cameras," Proc. of SPIE, 7662, 766212-1 (2010).